



Pal, A., Tan, C. M., & Beach, M. A. (2004). MIMO channels from multipath parameter extraction vs. direct measurements. (pp. 10 p). (COST 273), (TD (04) 016).

[Link to publication record in Explore Bristol Research](#)
PDF-document

University of Bristol - Explore Bristol Research

General rights

This document is made available in accordance with publisher policies. Please cite only the published version using the reference above. Full terms of use are available:
<http://www.bristol.ac.uk/pure/about/ebr-terms.html>

Take down policy

Explore Bristol Research is a digital archive and the intention is that deposited content should not be removed. However, if you believe that this version of the work breaches copyright law please contact open-access@bristol.ac.uk and include the following information in your message:

- Your contact details
- Bibliographic details for the item, including a URL
- An outline of the nature of the complaint

On receipt of your message the Open Access Team will immediately investigate your claim, make an initial judgement of the validity of the claim and, where appropriate, withdraw the item in question from public view.

EUROPEAN COOPERATION
IN THE FIELD OF SCIENTIFIC
AND TECHNICAL RESEARCH

COST 273 TD(04)016
Athens, Greece
2004/January/26-28

EURO-COST

SOURCE: Centre for Communications Research,
University of Bristol,
United Kingdom.

MIMO channels from multipath parameter extraction vs. direct measurements

A. Pal, C. M. Tan, and M. A. Beach
Centre for Communications Research
Room 2.19 Merchant Venturers Building
University of Bristol
Bristol BS8 1UB, UK.
Phone: + 44 117 954 5202
Fax: + 44 117 954 5206
Email: A.Pal@bristol.ac.uk

MIMO channels from multipath parameter extraction vs. direct measurements

A. Pal, C. M. Tan, and M. A. Beach

Centre for Communications Research
University of Bristol, UK.
Email: A.Pal@bristol.ac.uk

Abstract

This paper presents a capacity based analysis of directional Multiple-Input Multiple-Output (MIMO) channel measurements that were conducted with (16 x 16) element Uniform Circular Arrays (UCA) of patch antennas. The effect of antenna array configuration on performance has been investigated. A comparison between directly measured MIMO channels and MIMO channels generated from the multipath parameters that were extracted using the HS-SAGE algorithm is also presented.

1. Introduction

The theoretical performance benefits of deploying multiple antennas at both ends of a wireless communications link and the effect of correlation on MIMO capacity are well known [1-2]. Knowledge of the performance of measured MIMO channels in various indoor propagation scenarios and for different antenna configurations is of relevance to development of practical MIMO applications such as Wireless LANs operating in 5 GHz indoor channels for example. In order to evaluate the performance of these systems, realistic modelling of the indoor propagation channel as well as the antenna array is necessary. The model must be able to account for the wideband characteristics as well as the spatial domain properties of typical indoor environments. Channel measurements in relevant environments and wideband directional characterisation of these measured channels offer much knowledge that is needed for development of accurate channel models as well as understanding the interaction of the array geometry and element patterns with the environment.

The so called “double-directional” approach to characterisation of the wireless channel is well accepted as a comprehensive description of the channel [3]. Since the power-delay and directional properties are fully described at both the transmitter and receiver, double-directional channel data can be used to generate the wideband MIMO response for any given configuration of antenna arrays. Point to point double-directional data can also be obtained from other sources, for example Ray-tracing, stochastically from power delay profiles (PDP) and probability distributions of directions of arrival and departure, or from measurements.

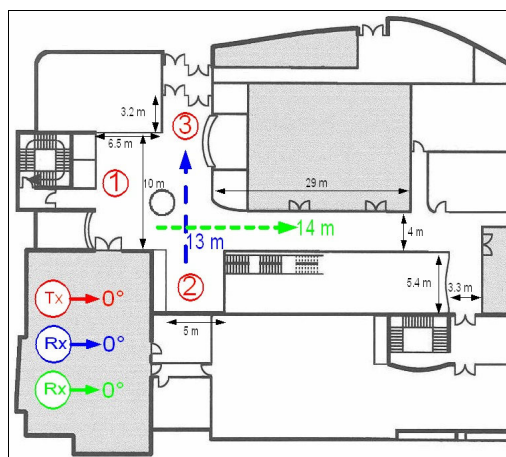
This paper presents a performance analysis of the channel measurements conducted with a (16 x 16) element Uniform Circular Arrays (UCA) of patch antennas. This antenna configuration made it possible to use the hybrid-space Space-Alternating Generalised Expectation-maximisation (HS-SAGE) algorithm [4] for the extraction of the power-delay and directional parameters of multipath components. The plane-wave propagation model was used to calculate MIMO channel response matrices from the

extracted multipath parameters. By choosing the antenna configurations in the model to match certain (4 x 4) element subsets of the measurement UCAs, a comparison was made between the measured MIMO channels and MIMO responses synthesised from extracted parameters.

2. Channel Measurements

2.1 Measurement Campaign

The measurement campaign was conducted alongside the MVCE campaign at the University of Bristol (UoB) [5]. The channel measurements were conducted using a Medav RUSK BRI channel sounder [6] capable of supporting multi-element wideband channel characterisation. The transmitter employs a periodic multi-tone signal with a bandwidth of 120 MHz, centred on 5.2 GHz and a repetition tone period of 0.8 μ s. The signal is constructed such that all tones have equal power and are evenly spaced over the measurement bandwidth. The patch antennas for the two identical 16-element UCAs were dual polarised (horizontal and vertical), and were designed by the Antennas Group at UoB [7]. Although they were dual-polarised, only the vertical polarisation was considered during the measurement. The UCAs had a radius of 1.28λ (at 5.2 GHz).



(1.a)



(1.b)

Figure 1.a: map showing locations of the Tx array and the dynamic paths of the Rx array.

Figure 1.b: the measurement set up in the Foyer of Merchant Venturers Building, UoB.

Dynamic measurements were conducted by slowly pushing the receiving UCA on a trolley, while the transmitting UCA was fixed at certain location. Measurements were taken under different propagation conditions. This includes line-of-sight (LOS), obstructed LOS, non-LOS, populated scenario, unpopulated scenario, and different antenna heights at either end. Measurements were conducted in several indoor environments, including the foyer, corridor, research lab, open plan office and outdoor court yard. However, only measurements from the foyer (Figure 1) have been used in this document.

2.2 Parameter Extraction

The newly developed HS-SAGE algorithm [4] was used to extract multipath parameters of the channel, i.e. Direction of Arrival (DoA), Direction of Departure (DoD), time delay of arrival, and Doppler shift. In brief, the HS-SAGE algorithm is a combination of the element-space and beamspace processing. Despite being suitable for use with a circular array, it also enhances the effective processing speed of the classical SAGE algorithm [8] without sensibly sacrificing accuracy and resolution. Each estimation of the multipath components was derived from five consecutive MIMO measurement snapshots.

Thus, from the measurements and parameter extraction processes described above, two descriptions of the wideband channel were obtained - the (16 x 16) measured wideband channel response of the UCAs, and a multipath component description of the channel (i.e. DoA, DoD, delay and power of each resolved ray).

3. Measurement Analysis

3.1 Channel Capacities of Measured Channels

When the power is allocated equally to each transmit element and frequency sub-channel, the capacity of the wideband frequency selective channel with overall bandwidth of W is given by:

$$C = \int_W \log_2 \left(\det \left(\mathbf{I}_N + \frac{\rho}{n_T} \mathbf{H}(f) \mathbf{H}^H(f) \right) \right) df \quad (1)$$

where $\mathbf{H}(f)$ is the normalised frequency response matrix of each narrowband sub-channel, ρ is the average SNR at each receiver branch over the entire bandwidth, and n_T is the number of transmitter. Here, it is assumed that power is distributed evenly amongst all transmit elements. The normalised capacity, C/W , of the wideband channel can be thought of as the mean of narrowband normalised capacities over the bandwidth W . For numerical evaluation of capacity of measured or simulated (synthesised) channels, capacity is more conveniently expressed in discrete form as

$$C = \lim_{\Delta f \rightarrow 0} \sum_{f=1}^{n_F} \Delta f \log_2 \left(\det \left(\mathbf{I}_N + \frac{\rho}{n_T} \mathbf{H}(f) \mathbf{H}^H(f) \right) \right) \quad (2)$$

where $n_F = W / \Delta f$, and Δf is the separation between adjacent frequency samples, and should be small enough to allow the assumption that the channel is flat in frequency over this range.

3.2 Channel Normalisation

The goal of channel normalisation is to scale a channel response so that the expectation of its power is unity. This is usually achieved by dividing a sufficiently large number of identically distributed channels by the square-root of their mean power. Each measured wideband snapshot $\mathbf{G}(t)$ of dimensions $(n_R \times n_T \times n_F)$ was

normalised separately. The channels were not normalised over time because the variance of capacity over time was not being investigated. Since any two adjacent elements in the array are spaced at $\sim 0.5\lambda$, they could be assumed to be sufficiently de-correlated, and therefore provide an adequate number of independent samples for normalisation.

When all the antenna elements within each of the arrays can be assumed to experience identical fading statistics, and the constituent Single-Input Single-Output (SISO) channels experience adequately independent fading, the normalisation coefficient, $\eta(t)$, can be calculated as that given in (3) :

$$\hat{\eta}(t)^2 = \frac{1}{n_R n_T n_F} \sum_{f=1}^{n_F} \sum_{j=1}^{n_R} \sum_{k=1}^{n_T} |g_{jk}(t, f)|^2 \quad (3)$$

and the normalised wideband channel response $\mathbf{H}(t)$ is given by (4):

$$\mathbf{H}(t) = \frac{\mathbf{G}(t)}{\hat{\eta}(t)} \quad (4)$$

However, since the measurements were taken with UCAs with directive patch antennas oriented in different directions, certain antenna elements were bound to experience greater mean pathloss than others. Applying equation (3) for normalising such a channel would result in poor estimate of $\eta(t)$, as it takes the average over all constituent SISO powers, from LOS to completely shadowed subchannels (a common scenario in double-directional measurement with full azimuth view at both ends). Therefore, for the case of partly shadowed arrays, a different approach to normalisation was used. The normalisation factor was taken to be the gain of the strongest constituent SISO subchannel, as given by (5).

$$\hat{\eta}(t)^2 = \max \left[\frac{1}{n_F} \sum_{f=1}^{n_F} |g_{jk}(t, f)|^2 \right], \quad \forall (j, k) : j = 1..n_R, k = 1..n_T \quad (5)$$

Since transmit power (measured at ~ 26 dBm) was fixed for all measurement scenarios, factoring out the maximum constituent SISO power effectively removes the pathloss caused by the relative locations of transmit and receive arrays. Equations (3) and (5) will therefore be referred to as *uniform* and *maximum-power normalisation* respectively in the remainder of this document. The results of these two normalisation approaches for different antenna configurations are discussed in section 3.3.2. It was found that (3) is ideally applicable only when all the receive elements experience the same shadowing, otherwise (5) might be preferred.

3.3 Candidate Antenna Arrays

The purpose of the (16 x 16) element measurements was to fully characterise the Power Azimuth Spectra (PAS) for given propagation scenarios in full azimuth view. In order to aid comparison between direct measurements and MIMO channels synthesised from the multipath parameter based model (Section 4), the antenna configurations for the model were chosen to match certain (4 x 4) subsets of the (16 x 16) measurement arrays. A brief overview of these (4 x 4) channels is given below.

3.3.1 (4 x 4) Facing and Non-Facing MIMO sectors

Most measurements were conducted with the antenna arrays placed with line of sight of each other. However, due to the shape/construction/geometry of the arrays and the narrow beamwidth of the patch antennas deployed, only some of the transmit-receive antenna channel pairs experience a dominant LOS component.



Figure 2: UCAs of patch antennas. The broadside of each antenna is along the line of the radius.

Two (4 x 4) MIMO sectors were observed – one where the arrays face each other, and the other where the transmit and receive arrays pointed in opposite directions. From Figure 2, an example of *facing* antennas is (Tx 1 and Rx 9), and example of *non-facing* antennas is (Tx 9 and Rx 1). As expected, the *non-facing* sectors were found to exhibit Rayleigh fading, aided by the large number of scatterers present in the indoor environment. The *facing* arrays were found to follow a Ricean distribution (Figure 3). *Facing* and *non-facing* antenna sectors have been used to simulate LOS and NLOS MIMO scenarios in Section 4.

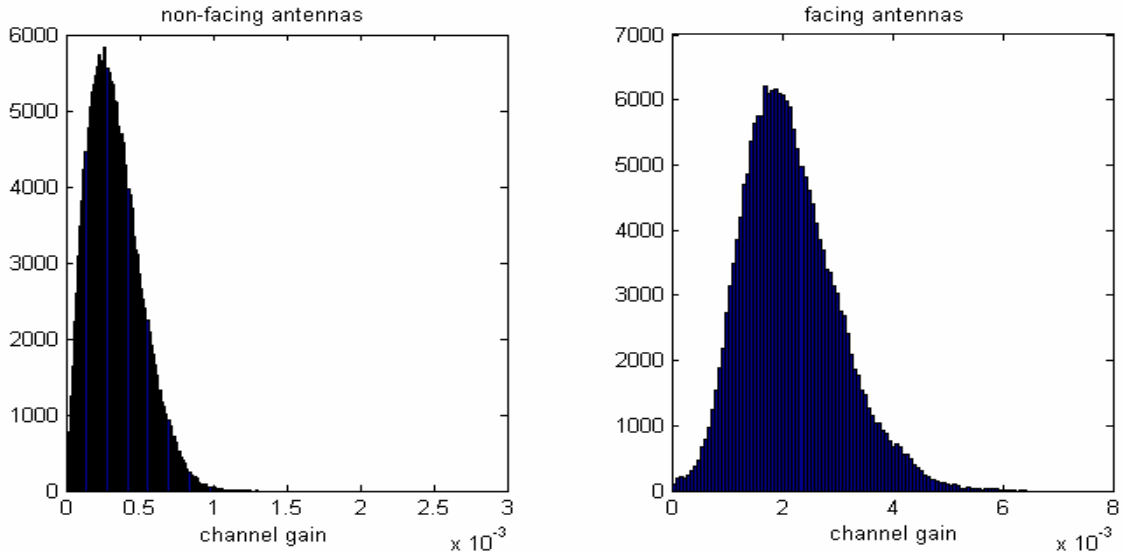


Figure 3: Channel gains of non-facing and facing (4x4) MIMO sectors, showing Rayleigh and Ricean fading

3.3.2 Adjacent-Antennas Arrays vs. Arrays with Opposite-End Antennas

From Figure 2, an example of (4 x 4) Adjacent-Antenna Arrays is antennas 1,2,3,4 in both arrays, whereas an example of Opposite-End-Antenna Arrays is antennas 1,5,9,13 in both arrays.

Figure 4 shows a capacity comparison between these two MIMO cases, for both types of normalisation approaches described in Section 3.2. As expected, *maximum power normalisation* (Equation 5) gives lower estimates of capacity than *uniform normalisation*. But the point to note here is that this discrepancy is more pronounced for the *opposite-end* antenna case, as the receive elements experience different levels of shadowing. If *uniform normalisation* were used here, the estimated pathloss would be much greater than the pathloss experienced by the antenna receiving the maximum power.

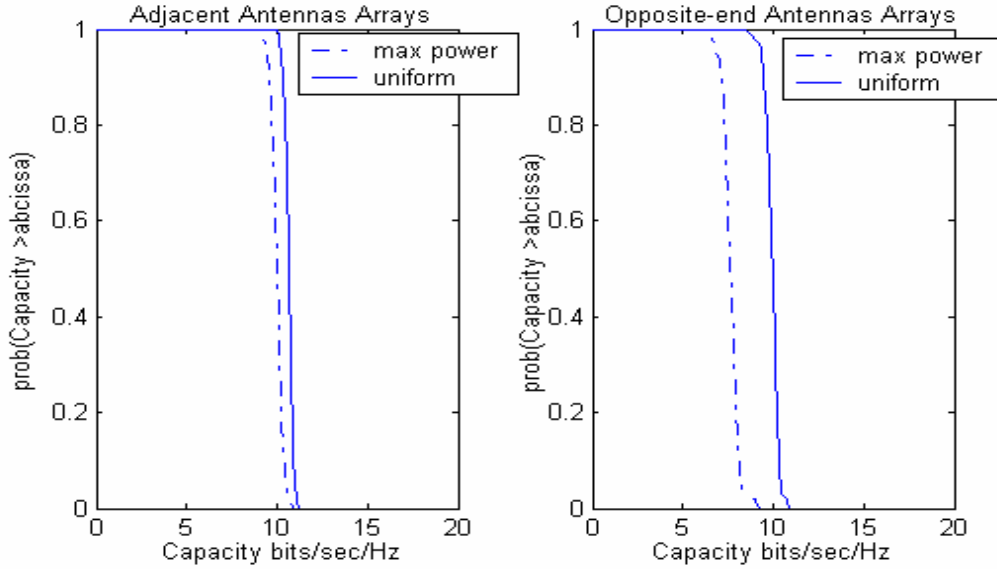


Figure 4: CCDFs of arrays with *adjacent* and *opposite-end* antennas, for two types of normalisation approaches.

The variation between the two normalisation approaches in the adjacent-antenna case is small, and can be attributed to the difference in orientation angle of 22.5° between any two adjacent antennas and the highly directional patterns of the patch antennas employed. Thus, the estimation of normalised capacity of arrays consisting of antennas oriented in different directions is sensitive to the normalisation process employed. This problem has a bearing on design of non-linear arrays employing directional antennas.

4. Extracted Parameters vs. Measurements

4.1 The plane-wave channel model

The double-directional approach to modelling MIMO channels [3] uses knowledge of joint distribution of time, directions of arrival and departure, and power (path gain) of multipath components to predict the channel response for arbitrary antenna arrays placed in the channel. The extracted multipath components describe the channel from the transmit origin (arbitrary reference point) to the receive origin, and the plane wave propagation assumption is made to calculate the fading response of each transmit-receive antenna pair, where the antennas are placed closed to the respective origin points.

The tap-delay response for each delay bin l ($l = 1..N_l$) is given by (6), and is similar to the model proposed by Xu in [9]. N_l was chosen to be equal to the number of frequency tones employed in the measurements. The subscript l has been omitted in the rest of the equation (from $P_{s,l}$ and $\theta_{s,l}$) for clarity. The spacing between delay bins is given by $[1/\text{measurement bandwidth}]$. For each channel snapshot, the extracted multipath components were assigned to the closest delay bin, depending on their excess delay. The wideband impulse response from each transmit element k to receive element j is given by the complex summation of all multipath components at each delay bin l .

$$h_{j,k,l} = \sum_{s=1}^{N_s} \sqrt{P_s} e^{j\phi_s} \sqrt{G^{Rx}(\underline{\theta}_s^A, \underline{\varphi}_j)} \sqrt{G^{Tx}(\underline{\theta}_s^D, \underline{\varphi}_k)} e^{j2\pi(\underline{x}_j^R \bullet \underline{\theta}_s^A)} e^{j2\pi(\underline{x}_k^T \bullet \underline{\theta}_s^D)} \quad (6)$$

where ($j = 1..n_R, k = 1..n_T$) and

N_s is the number of multipath components within each delay bin

P_s is the power of each multipath component

ϕ_s is the overall phase of each path, from Tx origin to Rx origin

$\sqrt{G^{Rx}}, \sqrt{G^{Tx}}$ the antenna pattern gain at receiver and transmitter respectively

$\underline{x}_j^R, \underline{x}_k^T$ locations of the receiving and transmitting elements w.r.t respective origins

$\underline{\theta}_s^A, \underline{\theta}_s^D$ directions of arrival and departure of each path

$\underline{\varphi}_j, \underline{\varphi}_k$ directions of orientation of the receiving and transmitting elements

The wideband channel response was calculated from discrete-Fourier transform (DFT) of the tap-delay response $h_{j,k,l}$. Since the above model makes the assumption that all propagation arrives in plane-waves during the measurement campaign, the antenna arrays were placed at sufficient separation distance from the nearest scatterers in order to prevent the effect of near field scattering. The model allows us to derive the channel response for any antenna array configuration (antenna patterns, placement of antennas, etc). The locations and orientations of antennas within the arrays were chosen to match some of the configurations described in Section 3.3.

4.2 Results: Extracted Parameters-based vs. Measured MIMO channels

The extracted multipath parameters were used in the model to generate channels for *facing* and *non-facing* arrays, which were shown to be equivalent to LOS and NLOS MIMO channels respectively in Section 3.3.1. The model was found to underestimate the normalised capacity, for both LOS and NLOS channels (Figure 5).

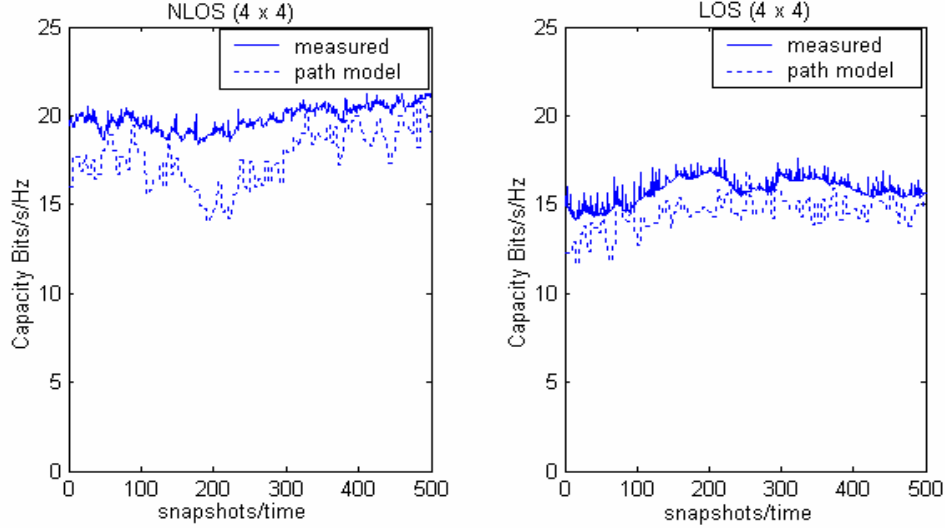


Figure 5: Capacities of NLOS and LOS channels for directly measured and multipath parameter generated MIMO channels

However, although the absolute capacities might be incorrect, the model correctly predicts the relative capacities between NLOS and LOS channels, i.e. the difference between LOS and NLOS capacity was found to be similar for the model generated and measured channels. Since all arrays consist of adjacently placed antennas pointed in similar directions, the normalisation given by equation (3) was used. Normalised LOS capacities are typically lower than NLOS because the dominant LOS component has the effect of correlating the MIMO subchannels.

If the parameter extraction process were completely accurate and given enough resolution (hardware limited though), we could expect the channels calculated from the model to match perfectly with measured channels because all parameters are known. But this is not the case. There are a few possible reasons for underestimation of capacity. Firstly, only the strongest 100 estimated multipath components were calculated whilst extracting parameters for each scenario. Also, in the model, only multipaths of power within 30 dB dynamic window (relative to the strongest estimated path) were used, ignoring all other relatively weaker paths. Note that due to the nature of the parameter estimation algorithm, estimates of the weak components might not be reliable and accurate.

The above comparison provides a validation of the plane-wave model for calculating MIMO channels from extracted multipath, and also the HS-SAGE multipath parameter extraction process. Given reliable directional characterisation of the channel, the correlation properties between the constituent subchannels is modelled with some accuracy. This makes the plane-wave model a useful tool for analysing the effect of antenna array configurations on performance in any given propagation environment.

5. Conclusions

A capacity analysis of directional MIMO measurements has been presented, and a comparison between measured channels and channels synthesised from extracted multipath components has been presented. This was a validation for using extracted parameters from the HS-SAGE algorithm in the plane-wave model. The plane-wave model could be a useful tool for design of antenna arrays that employ directional antennas, such as the patch antennas used here. As these arrays are more likely to experience shadowing across them, they may require a different normalisation process, like the one described earlier in the paper.

References

- [1] G. J. Foschini and M. J. Gans, 'On Limits of Wireless Communications in a Fading Environment when Using Multiple Antennas,' *Wireless Personal Communications*, pages 311-355, 1998.
- [2] D-S. Shiu, G. J. Foschini, M. J. Gans, and J.M. Kahn, 'Fading Correlation and its effect on the Capacity of Multi-Element Antenna Systems,' *IEEE International conference on Universal personal communications (ICUPC'98)*, vol. 1, pp. 429-433, October 1998.
- [3] M. Steinbauer, A. F. Molisch, and E. Bonek, 'The Double-Directional Radio Channel,' *IEEE Antennas and Propagation Magazine*, vol. 43, no. 4, pp. 51-63, August 2001.
- [4] C. M. Tan, M. A. Beach, and A. R. Nix, 'Multi-dimensional hybrid-space SAGE algorithm: Joint element-space and beamspace processing,' *IST Mobile and Wireless Communications Summit 2003*, Aveiro, Portugal, 15-18 June 2003.
- [5] M. A. Beach, C. M. Tan, and A. R. Nix, 'Indoor Dynamic Double Directional Measurements,' *International Conference on Electromagnetics in Advanced Applications*, Turin, Italy, 11 September 2003.
- [6] www.channelsounder.de, dated 10 January 2004.
- [7] D. L. Paul, I. J. Craddock, C. J. Railton, P. N. Fletcher, and M. Dean, 'FDTD analysis and design of probe-fed dual-polarised circular stacked patch antenna,' *Microwave and Optical Tech. Letters*, vol. 29, no. 4, pp. 223-226, May 2001.
- [8] B. H. Fleury, M. Tschudin, R. Heddergott, D. Dalhaus and K. I. Pedersen, 'Channel parameter estimation in mobile radio environments using the SAGE algorithm,' *IEEE JSAC*, vol. 17, pp. 434-449, March 1999.
- [9] H. Xu, D. Chizhik, H. Huang, and R. Valenzuela, 'A wave-based wideband MIMO channel modelling technique,' *PIMRC 2002*.